Effect of Temperature and Dynamic Loading on the Mechanical Properties of Copper-Alloyed High-Strength Interstitial-Free Steel

R. RANA, S.B. SINGH, W. BLECK, and O.N. MOHANTY

Crash resistance and formability relevant mechanical properties of a copper-alloyed interstitial-free (IF) steel processed under various conditions of batch annealing (BA), continuous annealing (CA), and postcontinuous annealing aging have been studied in a wide range of strain rate (3.33×10^{-4} to 200 s^{-1}) and temperature (-100 °C to $+20$ °C). These properties have been compared with similarly processed traditional mild and high-strength IF steels. Assessment of various parameters such as strength, elongation, strain rate sensitivity of stress, strain-hardening capacity, temperature sensitivity of stress, activation volume, and specific energy absorption of all these steels implies that copper-alloyed IF steel is soft and formable in CA condition. It can be made stronger and more crash resistant than the conventional mild- or high-strength IF steels when aged to peak strength after CA. Room-temperature strain rate sensitivity of stress of the investigated steels exhibits a two-stage behavior. Copper in solution in ferrite causes solid solution softening at low temperatures (≤ 20 °C) and at high strain rates (200 s^{-1}).

I. INTRODUCTION

INTERSTITIAL-FREE (IF) steels are widely used for auto body applications because of their high formability (strain-hardening exponent $n \geq 0.22$ and Lankford parameter $r_m \geq 1.8$).[1,2] With modern degassing and decarburization techniques, the total C and N content is limited to less than ~0.004 wt pct each in these steels. In addition, IF steels contain small amounts of stabilizing elements such as Ti and/or Nb to scavenge out the interstitial atoms from the solid solution in the form of precipitates such as carbides, nitrides, sulfides, carbonitrides, and carbosulfides.[3–5] The biggest disadvantage of IF steels is their low strength (tensile strength ≤ 360 MPa). Attempts have been made to improve the strength of IF steels using metallurgical concepts such as solid solution strengthening (by P, Mn, and Si), strain age hardening (bake hardening), Hall–Petch hardening, etc.[6] It is now possible to achieve strengths of up to 450 MPa in high-strength IF (IF-HS) steels and bake hardening steels.

Recently, a new type of IF steel has been reported with much higher strength levels (~460 MPa yield strength (YS) and ~575 MPa tensile strength) by addition of ~1.2 wt pct copper.[7] This copper-alloyed IF (IF-Cu) steel uses the classical precipitation hardening effect of copper in α iron.[8–11] It has been suggested that the high formability of IF steels would be used by press forming the IF-Cu steel in the as-annealed condition when it is soft and formable and then it can be aged to give rise to high strength.[7,12–14]

Crash resistance and lightweight structure have become the major design criteria for modern car bodies.[15] Mechanical properties of a material determined under dynamic loading conditions have a very close relationship with its crash resistance.[15] Crash resistance is often predicted through simulation programs, which require the material parameters such as strength, elongation, energy absorption, strain rate sensitivity of stress, etc. determined under dynamic loading conditions. Further, forming operations sometimes encounter much higher deformation rates than those used during determination of quasistatic mechanical properties. Therefore, to completely understand the behavior of the high-strength IF-Cu steels for automotive applications, it is important to study the dynamic mechanical properties.

The IF-Cu steel has been recommended to be used in car body based only on its high quasistatic tensile strength in peak-aged condition and good formability properties in continuous annealed (CA) condition.[7,12–14,16,17] The response of this material under dynamic loading conditions and its mechanical properties at subambient temperatures have not been reported yet. The present work therefore aims to determine the crash resistance and formability relevant mechanical

R. RANA, formerly DAAD Ph.D. Student, Department of Ferrous Metallurgy, RWTH Aachen University, D-52072 Aachen, Germany, is Researcher, Corus Research, Development and Technology, 1970 CA IJmuiden, The Netherlands. Contact e-mail: radhakanta.rana@corusgroup.com; r.rana@daad-alumni.de S.B. SINGH, Associate Professor, is with the Department of Metallurgical and Materials Engineering, Indian Institute of Technology Kharagpur, Kharagpur-721 302, India. W. BLECK Professor and Head of the Department, is with Department of Ferrous Metallurgy, RWTH Aachen University. O.N. MOHANTY, formerly Tata Research Professor, Department of Metallurgical and Materials Engineering, Indian Institute of Technology Kharagpur, is Vice Chancellor, Biju Patnaik University of Technology, Bhubneswar-751 003, Orissa, India.
Manuscript submitted July 18, 2008.
Article published online February 4, 2009.

properties of the IF-Cu steel by dynamic tensile tests under various processing conditions (batch annealing, continuous annealing, and postcontinuous annealing aging). These properties have been studied as a function of strain rate ranging from quasistatic to dynamic conditions (3.33×10^{-4} to 200 s^{-1}) and deformation temperature ranging from subambient temperature to room temperature (-100 °C to $+20$ °C). Further, all these mechanical properties have been compared with the conventional IF and IF-HS steels in order to assess the suitability of the IF-Cu steel for automotive applications.

II. EXPERIMENTAL DETAILS

A. *Material and Processing*

The IF-Cu steel with chemical composition presented in Table I was made in a semicommercial vacuum induction furnace and cast *in situ*. The ingots were reheated at 1200 °C in Ar atmosphere for 1 hour and then hot rolled into 4-mm-thick strips with a finish rolling temperature of 900 °C and cooled to room temperature in normal air. The hot-rolled strips were cold rolled into 0.8-mm thin sheets allowing ~80 pct thickness reduction. The sheets were then annealed in two schedules simulating the industrial batch and continuous annealing treatments. The CA and BA treatments were done in salt bath furnace at 820 °C for 1 minute and at 700 °C for 4 hours, respectively. Both annealing treatments resulted in completely recrystallized microstructure.[12] The CA IF-Cu steel was aged to peak-strength by aging at 550 °C in a salt bath furnace for 1 hour.[14]

In order to compare the properties of the IF-Cu steel, one traditional mild IF steel and two traditional IF-HS steel grades were also investigated. The compositions of these steels are listed in Table I along with that of IF-Cu steel. The mild IF steel, designated as IF steel, was received in industrial cold-rolled condition and was annealed in the salt bath furnace at 700 °C for 30 minutes and at 820 °C for 1 minute until complete recrystallization.

Table I. Chemical Composition of Investigated IF-Cu, Mild IF, and IF-HS Steels in Weight Percent

Elements	Steels			
	IF-Cu	IF	IF-HS-1	IF-HS-2
C	0.002	0.002	0.004	0.003
Mn	0.080	0.150	0.570	0.350
S	0.007	0.009	0.005	0.008
P	0.012	0.010	0.031	0.042
Si	0.023	0.007	0.010	0.011
Al	0.011	0.200	0.042	0.043
Cu	1.18	0.034	0.015	0.028
Cr	0.024	0.028	0.025	0.017
Ni	0.013	0.024	0.023	0.013
Nb	< 0.005	0.0005	0.0041	0.024
Ti	0.043	0.100	0.0828	0.023
N	0.0014	0.0056	0.0017	0.0026
Fe	balance	balance	balance	balance

Table II. Various Processing Conditions of Steels Tested under Dynamic Loading Conditions*

Treatment	Steel	Treatment Summary
BA	IF-Cu	700 °C, 240 min
	IF	700 °C, 30 min
CA	IF-Cu	820 °C, 1 min
	IF	820 °C, 1 min
	IF-HS-1	industrial CA
	IF-HS-2	industrial CA
CA + PA	IF-Cu	CA + (550 °C, 1 h)

*Annealing conditions resulted in complete recrystallization.[12]

A summary of the heat treatment (annealing and aging) schedules for various steels under this investigation is presented in Table II. Details of these heat treatments have been reported elsewhere.[12,14] The two IF-HS steels, designated as IF-HS-1 and IF-HS-2 steels, were procured in the industrial CA condition. While both steels are solution-strengthened by P and Mn, IF-HS-1 steel is stabilized by Ti only, whereas IF-HS-2 steel is dual-stabilized using both Ti and Nb.

B. *Test Procedure*

The dynamic uniaxial tensile tests were conducted using a servohydraulic 100 kN high-speed tensile testing machine (model: Schenk S56) at the Department of Ferrous Metallurgy (IEHK), RWTH Aachen University, which was a partner laboratory for preparing the "Recommendations for Dynamic Tensile Testing of Sheet Metals" published by the International Iron and Steel Institute (IISI).[18] The present experiments were in conformity with the draft standard for dynamic tensile testing worked out by European Structural Integrity Society (ESIS),[19] German Iron and Steel Institute (VDEh),[20] and the IISI.[18] The tests were done on 20-mm gage length flat longitudinal tensile specimens of as-received IF-HS steels and IF-Cu and IF steels processed under various conditions. For each specimen, three tests were done and the average values are reported. The initial strain rates for room-temperature (20 °C) tests were selected as 1, 20, 100, and 200 s^{-1} to determine the effect of strain rate on the mechanical properties. To investigate the effect of temperature on the mechanical properties, dynamic tensile tests with an initial strain rate of 200 s^{-1} were carried out at room temperature and at two subambient temperatures of -40 °C and -100 °C.

The high-speed tensile testing machine used in this study is capable of ram speeds in the range of 0.01 to 5000 mm s^{-1}. A temperature chamber enables tensile tests within the temperature range of -180 °C to $+180$ °C. While the high temperatures are created by inductive heating, the subambient temperatures are achieved by liquid nitrogen cooling. The force measurement during the tests was done using a titanium load cell directly on the sample. The piston displacement for the estimation of strain was recorded *via* a linear variable differential transformer placed directly on the sample and the results were verified with an electro-optical

extensometer. The storage of test data was done using a four channel transient recorder (sampling rate 1 MHz, 10 bit analogue-digital) and also on a personal computer for further analysis.

To evaluate the results, the recorded force and displacement data were converted into engineering stress-strain diagrams. At high strain rates, large fluctuations in the force signals caused by the inertia of the test equipment made the direct determination of the characteristic values very difficult. Therefore, a cubic spline was employed on the stress-strain diagram to approximate the unfiltered signal. To minimize errors due to exaggerated oscillation in the beginning of the test, YS of the specimens was determined for 1 pct strain, rather than 0.2 pct offset strain as is usually done in case of quasistatic tensile test. Energy absorption was determined from the area under the stress-strain curve until fracture. The area was calculated by integrating the stress-strain curve with respect to strain. To exclude the influence of specimen thickness, total energy values were normalized to mass specific values.

Room-temperature quasistatic uniaxial tensile tests on various steel samples with 25-mm gage length were also carried out a in a 25 kN tensile testing with a strain rate of 3.33×10^{-4} s^{-1} following DIN 10002 standard to compare the results with those obtained from dynamic loading conditions. The stress at 0.2 pct offset strain was considered as quasistatic YS. In addition, stress at 1 pct strain was also determined for direct comparison with the YS determined from dynamic tensile tests. To determine the anisotropy factors, samples were prepared in longitudinal (0 deg), diagonal (45 deg), and perpendicular (90 deg) to the rolling direction. The normal anisotropy factor (r_m) and planar anisotropy factor (Δr) were determined using their well known formula.[21] The strain-hardening exponent (n) was calculated using Hollomon equation[22] for the true strain range of 8 to 10 pct.

III. RESULTS AND DISCUSSION

The room-temperature quasistatic mechanical properties of the steels under various processing conditions are presented in Table III. As can be seen, IF-Cu steel is softer than the IF-HS steels (IF-HS-1 and IF-HS-2

steels) in CA condition as evidenced by their YS and ultimate tensile strength (UTS) values. The IF-Cu steel in CA condition possesses a higher strain-hardening exponent n and a slightly lower Lankford parameter r_m than the IF-HS steels. This IF-Cu steel when aged to peak strength is much stronger than the IF-HS steels due to the presence of nanometric copper precipitates.[23,24] These characteristics of quasistatic mechanical properties indicate that the IF-Cu steel can be press formed in CA condition when it is soft and formable and then it can be hardened efficiently during a postannealing aging treatment.[12-14] However, n and r_m values of IF-Cu steel are inferior to those of IF steel. Detailed documentations of these quasistatic mechanical properties have been reported previously.[12]

The deformation of materials at high strain rates is an adiabatic process, because the heat generated during deformation process cannot dissipate out of the sample during the test due to short testing duration.[25] Thus, the mechanical properties at high strain rates presented subsequently are influenced by this adiabatic heating as well. However, adiabatic heating in ultra-low-carbon steels such as the present ones is expected to be low due to their high thermal conductivity in the absence of large concentration of alloying elements.[26] Therefore, the results from different samples can be compared, assuming that the adiabatic effect is low and similar in all of them.

As described in Section II-B, large fluctuations in force signals in dynamic tensile tests were observed resulting in considerable oscillation in stress values. As a representative case, Figure 1 shows the representative raw and smoothened flow curves of CA IF-HS-2 steel for various strain rates. It can be observed that the oscillation of the stress is very periodic and the oscillation increases with increasing strain rate.

A. Effect of Strain Rate

1. Behavior of stress
Room-temperature flow curves of differently processed steels tested at various strain rates are presented in Figure 2. As the strain rate increases, true stress at a particular true strain increases for all the samples. Both room-temperature YS and UTS of the samples also increase as the strain rate increases (Figure 3) due to an

Table III. Quasistatic Mechanical Properties of the Investigated Steels at a Strain Rate of 3.33×10^4 s^{-1}*

Steel	Treatment Condition	YS, MPa	UTS, MPa	ε_u, Pct	ε_t, Pct	n_{8-10}	r_m	Δr
IF-Cu	BA	215	353	15	17.6	0.18	1.2	0.0
	CA	181	365	24.2	36.4	0.29	1.4	−0.1
	CA + PA	453	566	14.1	20.7	0.17	1.2	0.2
IF	BA	122	311	28	42.8	0.30	1.7	0.3
	CA	106	294	29.4	45.0	0.32	1.9	0.6
IF-HS-1	CA	215	357	24.0	38.9	0.22	1.8	−0.2
IF-HS-2	CA	225	374	23.2	36.3	0.22	1.6	0.0

*YS, UTS, ε_u, ε_t, n_{8-10}, r_m, and Δr are yield strength, ultimate tensile strength, uniform elongation, total elongation, strain-hardening exponent for the true strain range 8 to 10 pct, normal anisotropy factor, and planar anisotropy factor, respectively. The values of YS, UTS, ε_u, ε_t, and n_{8-10} are for the longitudinal specimen. The abbreviations BA, CA, and CA + PA are defined in text.
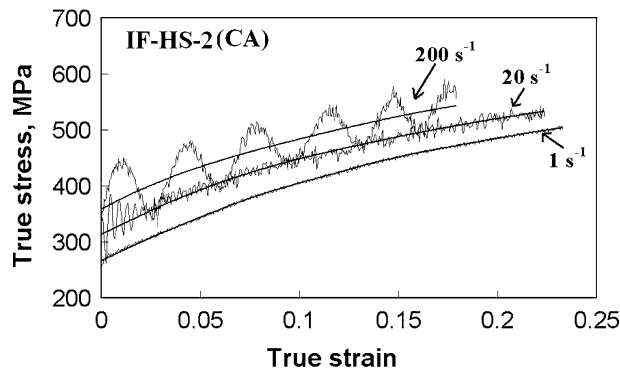
Fig. 1—Representative raw (with fluctuation of stress) and smoothened (without fluctuation of stress) flow curves of IF-HS-2 steel at room temperature determined from the dynamic tensile tests. Material was in CA condition. Fluctuation of stress increases as the strain rate increases.

increase in the dislocation density contribution to deformation.[27] For like-to-like comparison, the YS considered here for the quasistatic tensile tests (strain rate $\dot\varepsilon = 3.33 \times 10^{-4}\,\mathrm{s}^{-1}$) was also taken as the stress value at 1 pct strain, such as in the case of dynamic tensile tests (Section II–B). The extent of change in these strength levels for the materials in different conditions is different, as is analyzed later through room-temperature strain rate sensitivity of stress (m).

Continuous annealed and peak-aged (CA + PA) IF-Cu steel shows the highest YS and UTS followed by batch annealed (BA) IF-Cu steel at all the strain rates. The CA and BA IF steels have the lowest strength. The IF-Cu steel in CA + PA condition is expected to exhibit the highest strength since it contains copper precipitates in peak-aged condition.[23,24] The IF-Cu steel in CA condition has lower strength than CA IF-HS-1 and IF-HS-2 steels. This is understandable since IF-Cu steel, continuous annealed at 820 °C, has the entire amount of copper in solid solution.[12] Copper is a weak solid solution strengthener in ferrite when compared with P and Mn.[28] The IF-Cu steel, however, picks up strength when the CA material is aged at 550 °C for 1 hour. As previously discussed, this behavior of strength indicates that IF-Cu steel can be press-formed in CA condition when the material is soft and then hardened by a short time aging treatment to a strength level that is much higher than traditional IF-HS steels. The mild IF steel does not contain any major strengthening or precipitating element (Table I), and therefore has the lowest strength among the investigated steels.

The dependence of flow stress σ on the strain rate $\dot\varepsilon$ at a specific temperature T can be described using the extended Hollomon equation:[29,30]

$$\sigma = K \cdot \varepsilon^n \cdot \dot\varepsilon^m |_T \qquad [1]$$

where K is a constant similar to the strength coefficient of the material, ε is the true strain, n is the strain-hardening exponent, and m is the strain rate sensitivity of stress. At a constant true strain ε, Eq. [1] can be simplified to

$$\log \sigma = (C_1 + m \cdot \log \dot\varepsilon)|_{T,\varepsilon} \qquad [2]$$

where C_1 is a constant which is equal to log ($K\varepsilon^n$). A log σ – log $\dot\varepsilon$ plot should ideally yield a straight line, the slope of which is strain rate sensitivity of stress m. Such analysis was done for all steels under all investigated heat treatment conditions and the results are presented in Figure 4. As mentioned previously, T was 20 °C (room temperature) and σ at 1 pct ε ($\sigma_{0.01}$) was considered for the analysis. It was found that most of the steels show a two-stage m behavior over the experimented range of strain rate (Figure 4). The change in m value occurs at the strain rate of 1 s^{-1}. However, IF-Cu steel in CA condition is marked by a single m value for the whole range of strain rate. The two-stage m values (m_1 and m_2), along with the average m values (m_{av}) when the log σ – log $\dot\varepsilon$ data were fitted in the entire range of strain rate, are listed in Table IV. The m_{av} values for the present steels are in the same range as those for plain carbon steels.[31] Table IV further shows that for the steels showing the two-stage m behavior, the second stage m (m_2) is greater than the first stage m (m_1) suggesting a higher room-temperature strain rate sensitivity of stress of these steels at high strain rate ranges (>1 s^{-1}). The IF steel in CA condition shows the highest m_{av} followed by the same material in BA condition and IF-Cu steel in CA condition, while IF-Cu steel in CA + PA condition has the lowest m_{av}. The m_{av} value of BA IF-Cu steel is comparable with that of IF-HS steels in CA condition. The same observations are more or less true for m_1 and m_2 values. Further, it is to be mentioned for IF-Cu steel that room-temperature strain rate sensitivity of stress is higher when all amount of copper is in solid solution (CA condition) and it decreases as copper precipitates out (BA, CA + PA conditions).

The high room-temperature strain rate sensitivity of stress of IF-Cu steel in CA condition, which is comparable with that of the mild IF steel, suggests that IF-Cu steel in CA condition has high plasticity and therefore is easily formable. As mentioned previously, this fact supports the design philosophy of IF-Cu steel that it would be formed in soft annealed condition and then would be aged to high strength.

Plastic deformation in metals and alloys is a thermal activation process, which serves as the rate-controlling mechanism. The activation energy of plastic flow of a material is directly proportional to the activation volume v^* which is expressed as[32,33]

$$v^* = kT \left(\frac{\delta(\log \dot\varepsilon)}{\delta\sigma} \right)_T \qquad [3]$$

where k is the Boltzmann constant ($= 1.38 \times 10^{-23}$ JK^{-1}). Using this equation, activation volume at room temperature for the present steels under various treatment conditions has been calculated with $\sigma_{0.01}$ values from the flow curves in Figure 2. The v^* values in Table IV indicate that IF-Cu steel in CA + PA condition is the most difficult to deform requiring a high activation energy, while the same steel in CA condition can be deformed as easily as the mild IF steel in its BA or CA condition. This again corroborates the fact that
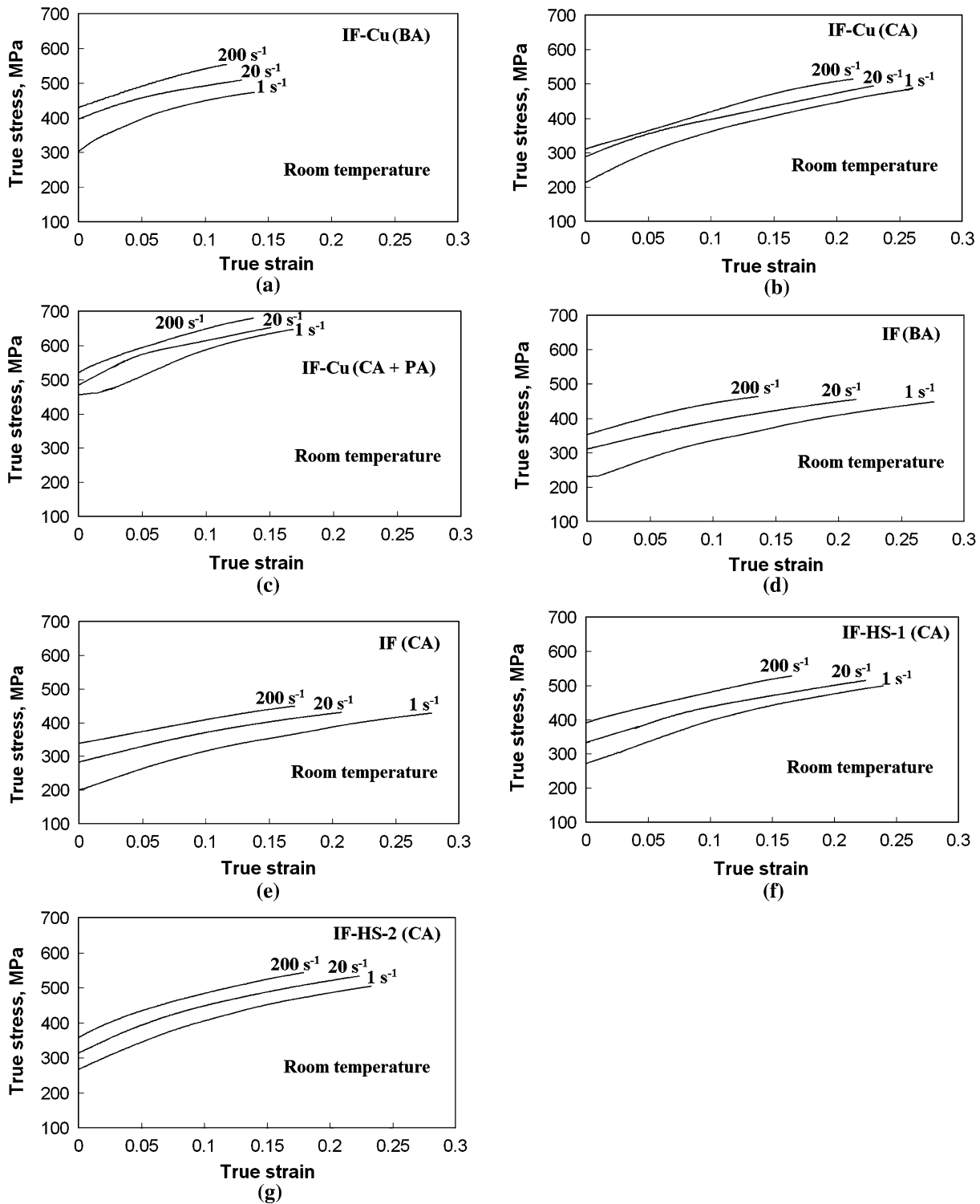
Fig. 2—Flow curves of different steels in different processing conditions tested at room temperature and at various strain rates. (*a*) IF-Cu steel in BA condition, (*b*) IF-Cu steel in CA condition, (*c*) IF-Cu steel in CA + PA condition, (*d*) IF steel in BA condition, (*e*) IF steel in CA condition, (*f*) IF-HS-1 steel in CA condition, and (*g*) IF-HS-2 steel in CA condition.

IF-Cu steel in CA condition can be formed easily, but it offers greater resistance to deformation in its final peak-aged condition indicating a high crash resistance. Moreover, IF-Cu steel in CA + PA condition has a higher v^* value than even the IF-HS steels. Table IV

also shows that the room-temperature activation volume increases with increasing copper precipitation in IF-Cu steel. Thus, v^* value is highest in CA + PA condition followed by BA and then CA conditions of IF-Cu steel.
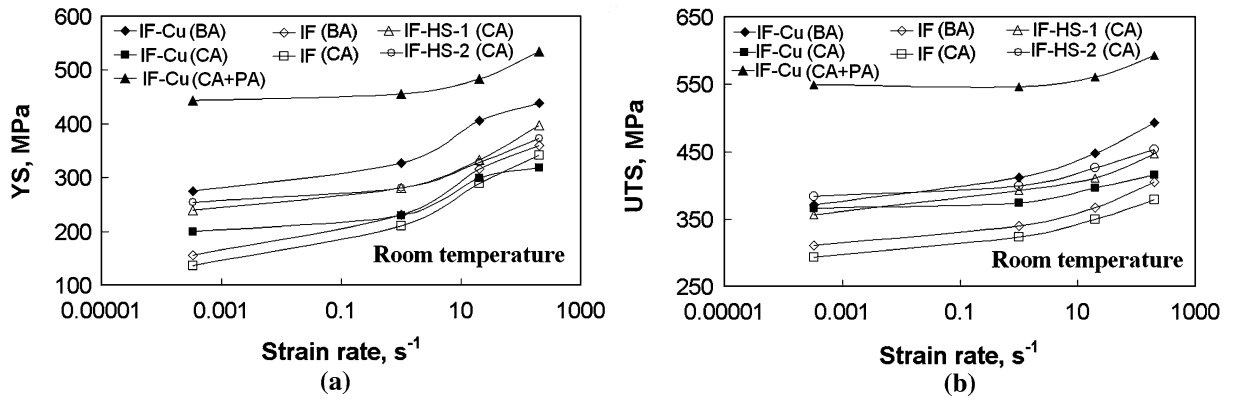
Fig. 3—Effect of strain rate on room-temperature strength values of steels processed under various conditions: (a) YS and (b) UTS. YS values correspond to the stress value at 1 pct strain.
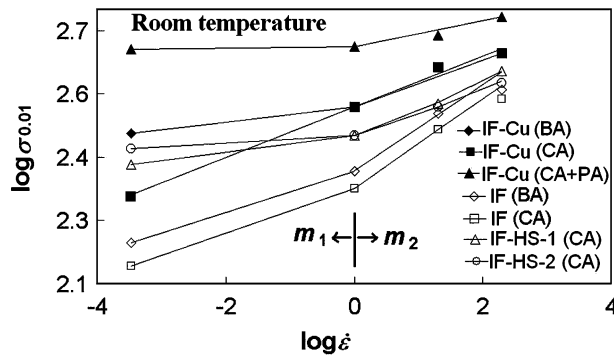

Fig. 4—Two-stage behavior of strain rate sensitivity of stress m at room temperature of steels processed under various conditions. First stage m value (m_1) corresponds to the strain rate range of 3.33×10^{-4} to 1 s^{-1} and the second stage m value (m_2) corresponds to the strain rate range of 1 to 200 s^{-1}. IF-Cu steel in CA condition reveals a single m value.

The average strain rate sensitivity of stress (m_{av}) and the activation volume (v^*) of the present steels, both at room temperature, are plotted as a function of quasi-static yield ratio (YS/UTS from the quasistatic tensile tests, Table III) in the composite graph of Figure 5. An almost linear dependence, with slopes of opposite sign, of the two factors on the quasistatic yield ratio can be seen for these IF steels. Yield ratio is inversely related to

the strain-hardening capacity of a material.[30] The m_{av} increases as the quasistatic yield ratio decreases and v^* increases as the quasistatic yield ratio increases. Further, m_{av} increases as v^* decreases for these steels.

2. Strain hardening

The variation of room-temperature yield ratio (YS/UTS) with strain rate for the investigated steels treated in different conditions shown in Figure 6. Yield ratio increases sharply from quasistatic condition to 20 s^{-1}; thereafter, it increases gradually for all steels in all treatment conditions. Since strain-hardening capacity is inversely related to yield ratio,[30] this trend indicates that strain-hardening capacity of these steels decreases sharply as the deformation rate changes from quasistatic to dynamic situation. The lowest yield ratio of IF-Cu steel in CA condition at high strain rates (>1 s^{-1}) suggests its highest strain-hardening capacity among the investigated steels at dynamic strain rates. This implies that IF-Cu steel in CA condition can be formed more efficiently in stretching situation than conventional IF and IF-HS steels. This behavior would lead to a more delayed necking of CA IF-Cu steel, because the material would strain harden as it thins down.

3. Elongation

The uniform elongation at room temperature for all the materials in different treatment conditions decreases

Table IV. Room-Temperature Strain Rate Sensitivity of Stress m, Activation Volume v^* at Room Temperature, and Temperature Sensitivity of Stress n_a at Strain Rate of 200 s^{-1} of Steels Processed under Various Conditions**

Steel Samples	m_1	m_2	m_{av}	v^*, 10^{-22} m^3	n_a
IF-Cu (BA)	0.02	0.06	0.03	1.34	0.59
IF-Cu (CA)	—	—	0.06	1.09	0.90
IF-Cu (CA + PA)	0.002	0.03	0.01	2.07	0.71
IF (BA)	0.05	0.08	0.06	1.08	1.14
IF (CA)	0.05	0.09	0.07	1.09	1.02
IF-HS-1 (CA)	0.02	0.07	0.04	1.35	1.01
IF-HS-2 (CA)	0.01	0.05	0.03	1.78	1.07

**m_{av} is the average m value for the whole range of strain rate; and m_1 and m_2 are the m values determined in the strain rate ranges of 3.33×10^{-4} to 1 s^{-1} and 1 to 200 s^{-1}, respectively. The v^* values were determined in the strain rate range of 3.33×10^{-4} to 200 s^{-1}. The n_a values were determined in the temperature range of -100 °C to $+20$ °C. Abbreviations BA, CA, and CA + PA are defined in text.
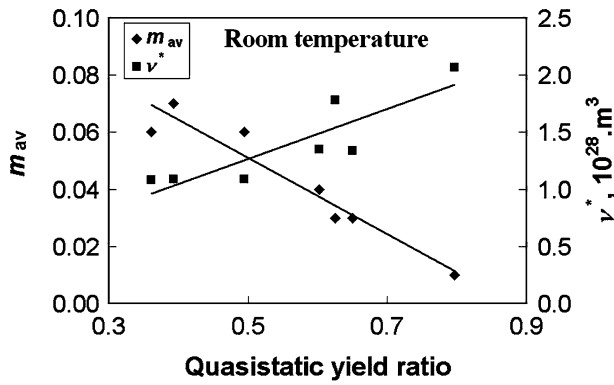
Fig. 5—Dependence of the average strain rate sensitivity of stress m_{av} and the activation volume v^*, both at room temperature, on the quasistatic yield ratio (ratio of yield strength to tensile strength) of the steels processed under various conditions and tested in the strain rate range of 3.33×10^{-4} to 200 s^{-1}. Strain rate of the quasistatic tensile test was 3.33×10^{-4} s^{-1}.
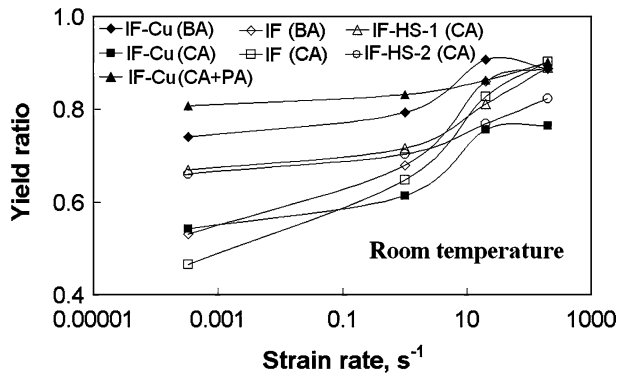

Fig. 7—Variation of room-temperature uniform elongation of steels processed under various conditions with strain rate.

Fig. 6—Variation of room-temperature yield ratio (YS to tensile strength ratio) with strain rate of steels processed under various conditions.

Fig. 8—Variation of specific energy absorption until 10 pct uniform strain E_{10} as a function of strain rate for steels processed under different conditions and tested at room temperature.

with the increasing strain rate (Figure 7). The elongation values from the quasistatic tensile tests have been excluded from Figure 7, as the gage length used in quasistatic and dynamic tensile tests were not the same (Section II–B). It is to be noted from Figure 7 that the drop in uniform elongation with increase in strain rate is not linear for all materials under different treatment conditions. Comparatively high-strength steels (IF-Cu steel in BA and CA + PA conditions) show a linear relationship between uniform elongation and strain rate, while the softer steels exhibit a nonlinear relationship. Further, the change in uniform elongation in softer steels is much higher than that in stronger steels. This can be attributed to the presence of stronger barriers to dislocation flow in stronger materials.[27]

4. Energy absorption

The energy absorbed up to a particular uniform elongation is more important than the total energy absorbed for automotive steels.[29] This is a very reasonable hypothesis because design aspects always consider a factor of safety rather than complete fracture of the material. In addition, the influence of adiabatic
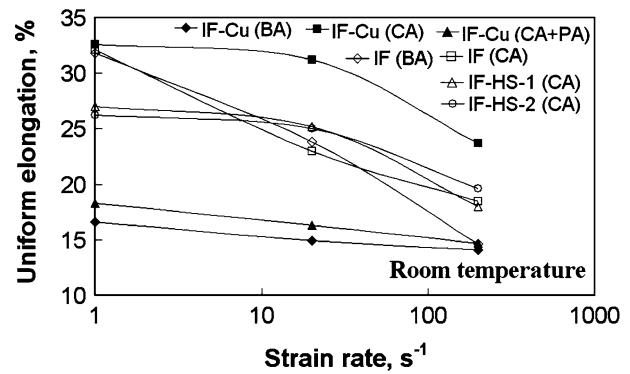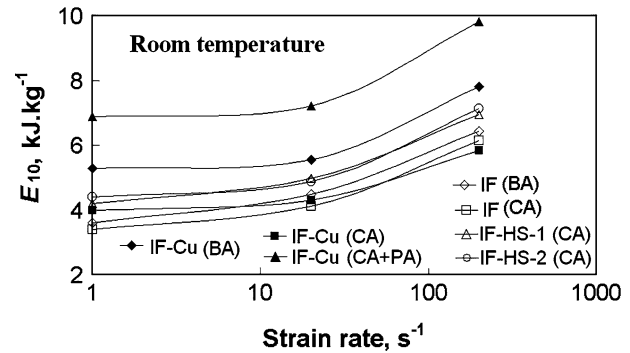
heating and statistical scatter in total elongation values would be less important with this approach. Therefore, the specific energy absorption at room temperature until 10 pct uniform elongation (E_{10}) at different strain rates was calculated for the steels and the results are shown in Figure 8. It can be observed that for all materials under all treatment conditions, E_{10} exhibits a linear increase with increase in strain rate. The reason could be the increase of stress levels with increase in strain rate as was observed in Figure 3. The IF-Cu steel in CA + PA condition shows ~80 pct higher E_{10} value than traditional IF steels including the IF-HS steels. This indicates a high crash resistance of this material. The IF-Cu steel in BA condition also shows a high E_{10} value at all experimented strain rates. However, it can be recalled that its formability parameters were found to be poor (Table III).

B. Effect of Temperature

1. Behavior of stress

Figure 9 shows the effect of temperature on the flow curves of the steels tested at a strain rate of 200 s^{-1}. It can be observed for all the steels processed under different conditions that the true stress increases at a particular true strain with lowering of temperature.
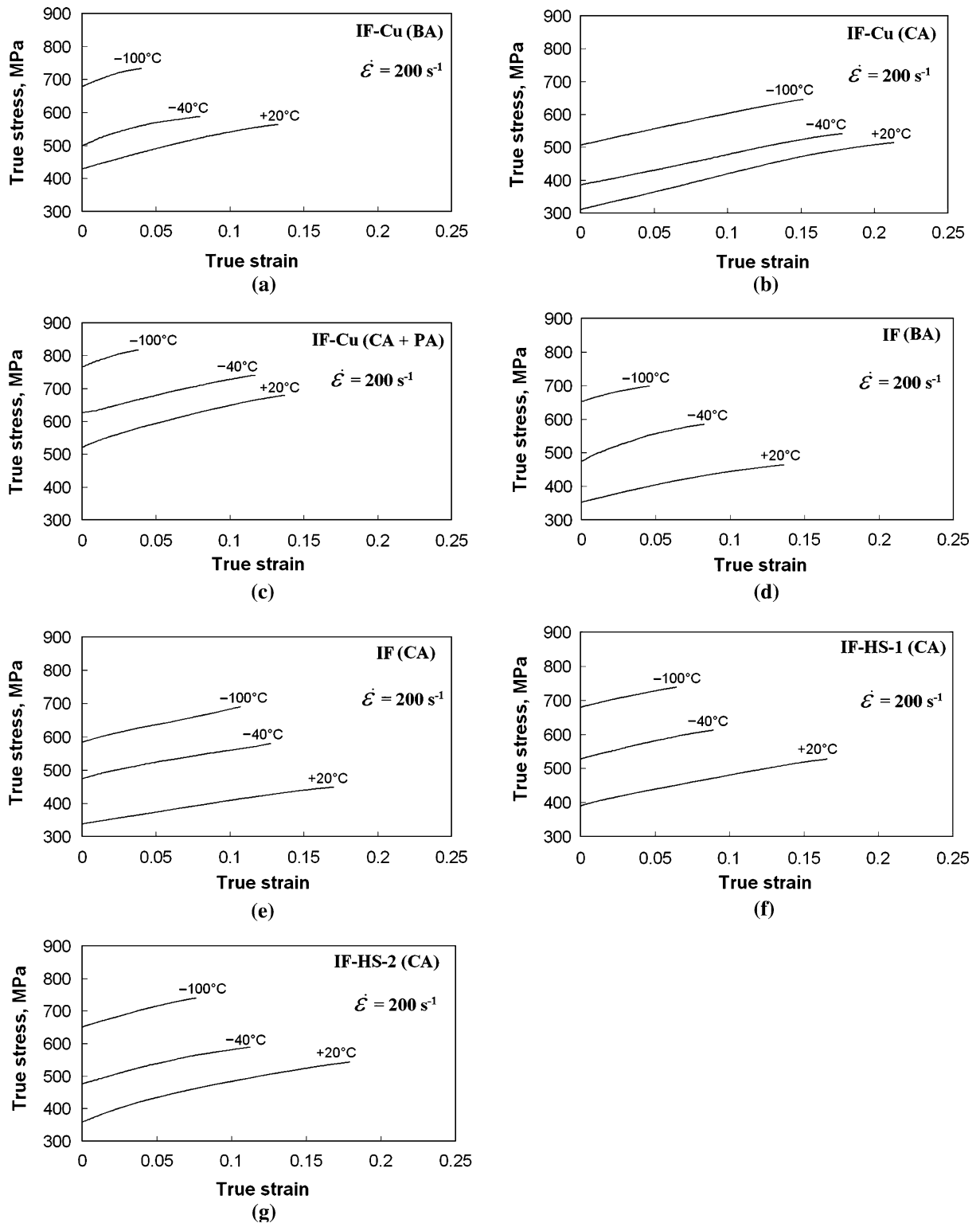
Fig. 9—Flow curves of steels processed under various conditions and tested with strain rate $\dot{\varepsilon}$ of 200 s^{-1} at various temperatures (*a*) IF-Cu steel in BA condition, (*b*) IF-Cu steel in CA condition, (*c*) IF-Cu steel in CA + PA condition, (*d*) IF steel in BA condition, (*e*) IF steel in CA condition, (*f*) IF-HS-1 steel in industrial CA condition, and (*g*) IF-HS-2 steel in industrial CA condition.

The effect of temperature on the YS and UTS of the steels at the strain rate of 200 s^{-1} is shown in Figure 10. As the temperature decreases, the strength values increase due to higher thermal activation barrier against material flow at lower temperatures.[27] The IF-Cu steel in CA + PA condition shows the highest YS and UTS at all temperatures due to the presence of peak-aged copper precipitates.[23,24] Continuous annealed IF-Cu
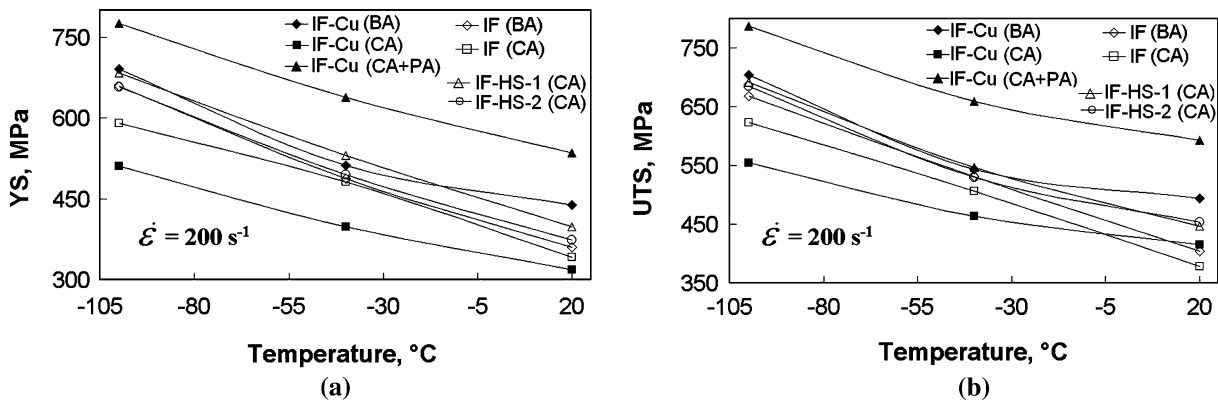
Fig. 10—Effect of temperature on (a) YS and (b) UTS of the steels processed under different conditions and tested at strain rate $\dot{\varepsilon}$ of 200 s^{-1}.

steel has the lowest YS at all temperatures and the lowest UTS at subambient temperatures. The strength values for other steels in various treatment conditions are in between the strength values of IF-Cu steel in CA and CA + PA conditions and both YS and UTS vary in a similar manner. The IF-HS steels show higher strength values than the IF steel in BA and CA conditions and IF-Cu steel in CA condition due to the solid solution hardening by P in IF-HS steels.[28]

The temperature sensitivity of stress n_a at specific true strain of ε and strain rate of $\dot{\varepsilon}$ can be quantified as[26]

$$n_a = \frac{-\log (\sigma_2/\sigma_1)}{\log (T_2/T_1)}\bigg|_{\varepsilon,\dot{\varepsilon}} \qquad [4]$$

where σ_1 and σ_2 are the true stresses at test temperatures T_1 and T_2, respectively, and $T_2 > T_1$. Equation [4] can be generalized as follows:

$$\log \sigma = (-n_a \log T + C_2)|_{\varepsilon,\dot{\varepsilon}} \qquad [5]$$

where C_2 is a material constant. Plot of $\log \sigma_{0.01}$ vs $\log T$ from Figure 9 according to Eq. [5] for various steels was made and the temperature sensitivity of stress n_a at the strain rate of 200 s^{-1} was determined by regression analysis. These n_a values are listed in Table IV. Unlike the two-stage m behavior over the investigated range of strain rate observed in Figure 4, a single value of n_a was obtained for all steels in all treatment conditions over the tested temperature range. The n_a values are higher for these ultra-low-carbon steels than for other normal carbon steels reported in literature (0.27 to 0.37).[31] The IF-Cu steel in all treatment conditions shows a lower temperature sensitivity of stress than the mild IF and IF-HS steels implying a smaller increase in strength with lowering of temperature.

Solute copper in ferrite causes solid solution softening at subambient temperatures and this effect becomes stronger at high strain rate deformation.[34] This characteristic is similar to that observed in Fe-Si, Fe-Ni, and Fe-Mn alloys.[35–38] It has been suggested that a decrease in Peierls stress due to the decrease in double kink nucleation energy by solute atom is responsible for the softening effect.[37,38] The lower temperature sensitivity of stress at the strain rate of 200 s^{-1} in IF-Cu steel can

probably be due to this softening effect. The IF-Cu steel in all three treatment conditions (BA, CA, and CA + PA) should contain variable amount of copper dissolved in the ferrite matrix[12] and the dissolved copper atoms should give rise to the softening effect.[34] However, the reason for the pronounced softening effect in IF-Cu steel in BA condition as reflected by its lowest n_a value in Table IV is not clear. The IF-Cu steel in BA condition should contain a lower amount of copper in solution than in CA condition;[12] therefore, in principle, the n_a value of the former should be higher. Copper-containing complex precipitates of (Fe, Ti, Cu, Si)P type have been reported to be present in BA IF-Cu steel.[12] The described anomaly suggests a possible effect of these copper-containing complex precipitates on the temperature sensitivity of stress of copper-containing steels. Further studies are clearly required to understand this anomaly. Moreover, it is interesting to note that the simultaneous presence of P and Mn in the IF-HS steels does not induce the softening effect, as is evident from their high n_a values comparable to that for mild IF steel (Table IV).

The n_a values at the strain rate of 200 s^{-1} calculated in the temperature of -100 °C to $+20$ °C (Table IV) were used to compute the YS of IF-Cu and IF steels at higher temperatures. The extrapolated curves for the variation of YS at a strain rate of 200 s^{-1} of IF-Cu and IF steels in CA condition are shown in Figure 11. It can be observed that they intersect at around 50 °C. This suggests that at a strain rate of 200 s^{-1}, copper causes solid solution hardening above 50 °C, whereas below this temperature, it causes softening in iron.

2. Strain hardening

The change in yield ratio as a function of temperature at the strain rate of 200 s^{-1} is shown in Figure 12 for the steels tested in variously treated conditions. Unlike a nonlinear dependence of yield ratio on strain rate at room temperature (Figure 6), the yield ratio increases almost linearly as the temperature decreases. A higher yield ratio obviously indicates a lower capacity of strain hardening of these steels at subambient temperatures. The IF-Cu steel in CA condition maintains its lowest value of yield ratio throughout the experimented
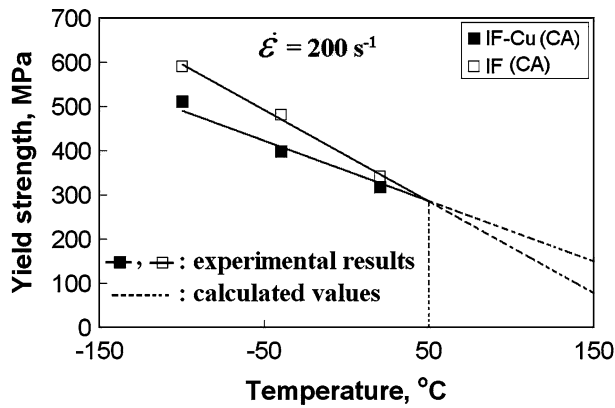
Fig. 11—Effect of solute copper on YS of IF steels at strain rate $\dot{\varepsilon}$ of 200 s^{-1}. Above 50 °C copper causes solid solution hardening and below 50 °C, it causes solid solution softening in iron. Experimental variation of YS is shown as solid continuous lines, whereas points denote the experimental values. Dotted lines signify extrapolation of the YS variation beyond the range of experimentation using the n_a values for the respective steels listed in Table IV.
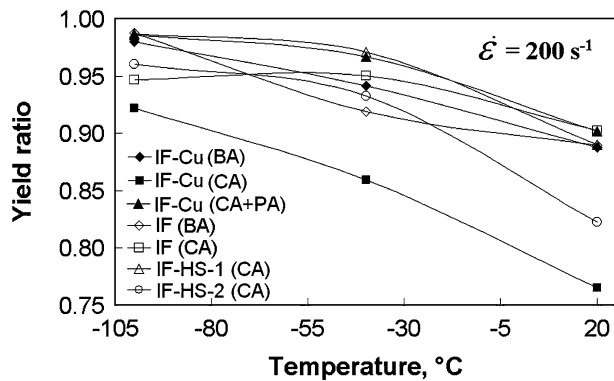

Fig. 12—Change in yield ratio (YS to tensile strength ratio) with temperature of steels processed under various conditions. Tensile tests were done at strain rate $\dot{\varepsilon}$ of 200 s^{-1}.

Fig. 13—Effect of temperature on uniform elongation of steels processed under various conditions. Tensile tests were done at strain rate $\dot{\varepsilon}$ of 200 s^{-1}.

Fig. 14—Variation of specific energy absorption until 10 pct uniform elongation (E_{10}) with temperature at strain rate $\dot{\varepsilon}$ of 200 s^{-1} for steels processed under various conditions.

temperature range, indicating its high capacity for strain hardening. Similar observation was made from Figure 6 as well for room-temperature tests under dynamic loading conditions.

3. *Elongation*

The effect of temperature on the uniform elongation of the variously treated steels at the strain rate of 200 s^{-1} is shown in Figure 13. A general trend of a decrease in the uniform elongation with decreasing temperature is observed for all the samples. The IF-Cu steel in CA condition shows the highest uniform elongation at all temperatures. The BA steels exhibit lowest uniform elongation at subambient temperatures.

4. *Energy absorption*

The E_{10} value (Figure 14) increases as the temperature falls for all samples tested at a strain rate of 200 s^{-1}. This is primarily due to an increase in the stress value with decrease in temperature as was seen in Figure 10. The IF-Cu steel in CA + PA condition absorbs higher
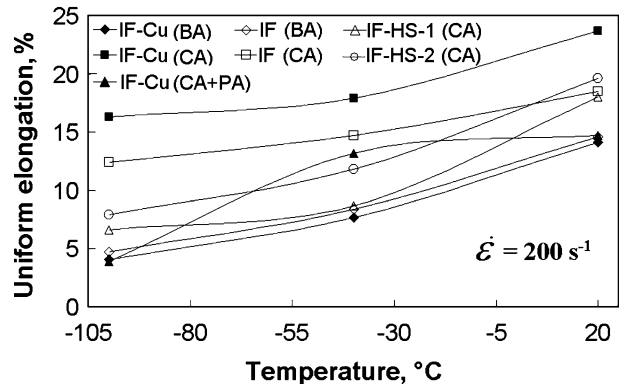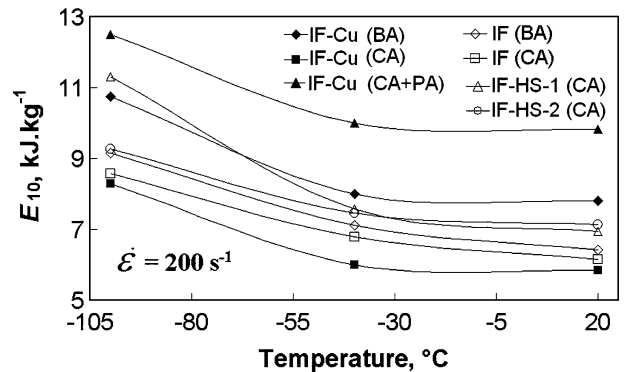
amount of energy than IF-HS steels and the mild IF steel at all the temperatures indicating a higher crash resistance of IF-Cu steel in CA + PA condition.

IV. CONCLUSIONS

Mechanical properties important for automotive applications of a copper-alloyed IF steel have been studied as a function of strain rate and temperature under various processing conditions and compared with traditional mild- and high-strength IF steels with similar processing history. The following conclusions can be drawn from the present work.

1. On the basis of strength, strain rate sensitivity of stress, strain-hardening capacity, elongation, and specific energy absorption determined from room-temperature high strain rate (up to 200 s^{-1}) tensile test, IF-Cu steel in CA condition appears to be a better material for forming purposes than traditional IF-HS steels. The IF-Cu steel in CA and peak-aged condition, on the other hand, is stronger and absorbs more energy than IF-HS steels indicating higher crash resistance.

2. The IF-Cu, IF, and IF-HS steels show a two-stage behavior of room-temperature strain rate sensitivity of stress with the change occurring at the strain rate of $1~\mathrm{s}^{-1}$. The first stage strain rate sensitivity is lower than the second stage value. A linear dependence of quasistatic strain-hardening capacity on the strain rate sensitivity of stress and activation volume was observed for these steels at room temperature.

3. The variation of strength values with decreasing temperature suggests that copper in solid solution in ferrite causes solid solution softening in IF-Cu steel below ~50 °C at a strain rate of $200~\mathrm{s}^{-1}$. However, the simultaneous presence of P and Mn in traditional IF-HS steels does not show this effect.

REFERENCES

1. S. Hoile: *Mater. Sci. Technol.*, 2000, vol. 16, pp. 1079–93.
2. H. Takechi: *ISIJ Int.*, 1994, vol. 34, pp. 1–8.
3. X. Yang, D. Vandershueren, J. Dilewijns, C. Standaert, and Y. Houbaert: *ISIJ Int.*, 1996, vol. 36, pp. 1286–94.
4. M. Hua, C.I. Garcia, and A.J. DeArdo: *Metall. Mater. Trans. A*, 1997, vol. 28A, pp. 1769–80.
5. M. Pricryl, Y.P. Lin, and S.V. Subramanian: *Scripta Metall. Mater.*, 1990, vol. 24, pp. 375–80.
6. T. Senuma: *ISIJ Int.*, 2001, vol. 41, pp. 520–32.
7. R. Rana, W. Bleck, S.B. Singh, and O.N. Mohanty: *Mater. Lett.*, 2007, vol. 61, pp. 2919–22.
8. E. Hornbogen and R.C. Glenn: *Trans. TMS-AIME*, 1960, vol. 218, pp. 1064–70.
9. S.R. Goodman, S.S. Brenner, and J.R. Low, Jr.: *Metall. Trans.*, 1973, vol. 4, pp. 2363–78.
10. N. Maruyama, M. Sugiyama, T. Hara, and H. Tamehiro: *Mater. Trans. JIM*, 1999, vol. 40, pp. 268–77.
11. A. Deschamps, M. Militzer, and W.J. Poole: *ISIJ Int.*, 2001, vol. 41, pp. 196–205.
12. R. Rana, W. Bleck, S.B. Singh, and O.N. Mohanty: *Steel Res. Int.*, 2007, vol. 78, pp. 612–21.
13. R. Rana, W. Bleck, S.B. Singh, and O.N. Mohanty: *Steel Res. Int.*, 2007, vol. 78, pp. 622–30.
14. R. Rana, W. Bleck, S.B. Singh, and O.N. Mohanty: *Steel Res. Int.*, 2007, vol. 78, pp. 631–37.
15. Vehicle Safety-ULSAB-AVC Crash Evaluations, ULSAB-AVC Consortium, Nov. 1999.
16. K. Kishida: *Nippon Steel Tech. Rep.*, 1995, No. 64, pp. 33–35.
17. Y. Hosoya, M. Morita, K. Tahara, and O. Fukumoto: *CAMP-ISIJ*, 1992, vol. 5, pp. 1823–26.
18. IISI Committee Report: Recommended Practice for Dynamic Tensile Testing for Sheet Metals, 2004.
19. ESIS Committee Report: Proposed Standard Method for Dynamic Tensile Tests: ESIS TC5, 1997.
20. German Steel Association (VDEh) Report: Dynamic Tensile Testing Recommendation, 2004.
21. W.T. Lankford, S.C. Snyder, and J.A. Bauscher: *Trans. ASM*, 1950, vol. 42, pp. 1197–1225.
22. G.E. Dieter: in *Mechanical Metallurgy*, McGraw-Hill, London, 1988, vol. p. 287.
23. G.M. Worral, J.T. Buswell, C.A. English, M.G. Hetherington, and G.D.W. Smith: *J. Nucl. Mater.*, 1987, vol. 148, pp. 107–14.
24. W.J. Phythian, S. Dumbill, P. Brown, and R. Sinclair: *Proc. 6th Int. Symp. on Environmental Degredation in Nuclear Power Systems–Water Reactors*, R.E. Gold and E.P. Simonen, eds., TMS, San Diego, CA, 1993, pp. 729–37.
25. H.C. Rogers: *Annu. Rev. Mater. Sci.*, 1979, vol. 9, pp. 283–311.
26. W.-S. Lee and C.-F. Lin: *Mater. Sci. Eng. A*, 1998, vol. 241, pp. 48–59.
27. H. Conrad and S. Frederick: *Acta Metall.*, 1962, vol. 10, pp. 1013–20.
28. L. Meyer, W. Bleck, and W. Müschenborn: *Proc. Int. Forum for Phys. Metall. of IF Steels*, ISIJ and Nissoh Iwai Corp., Tokyo, 1994, pp. 203–22.
29. W. Bleck and I. Schael: *Steel Res.*, 2000, vol. 71, pp. 173–78.
30. W. Bleck, P. Larour, and A. Bäumer: *Proc. 3rd Int. Conf. on Advanced Materials Processing (ICAMP-3)*, Institute of Materials Engineering, Australasia, Melbourne, 2004, pp. 21–29.
31. W.-S. Lee and C.-Y. Liu: *Mater. Sci. Eng. A*, 2006, vol. 426, pp. 101–13.
32. H. Conrad and H. Wiederisch: *Acta Metall.*, 1960, vol. 8, pp. 128–30.
33. L. Shi and D.O. Northwood: *Acta. Metall. Mater.*, 1995, vol. 43, pp. 453–60.
34. J. Syarif, T. Tsuchiyama, and S. Takaki: *ISIJ Int.*, 2003, vol. 43, pp. 1100–04.
35. W. Jolley: *Trans. AIME*, 1968, vol. 242, pp. 306–14.
36. W.C. Leslie, R.J. Soeber, S.G. Babcock, and S.J. Green: *Trans. ASM*, 1969, vol. 62, pp. 690–710.
37. Y.T. Chen, D.G. Atteridge, and W.W. Gerberich: *Acta Metall.*, 1981, vol. 29, pp. 1171–85.
38. K. Okazaki: *J. Mater. Sci.*, 1996, vol. 31, pp. 1087–99.